

Study of the current-driven, superconducting to normal transition

Jacob Szeftel¹, Nicolas Sandeau², and Michel Abou Ghantous³

¹ Laboratoire de Photonique Quantique et Molculaire, UMR 8537, Ecole Normale Supérieure de Paris-Saclay, CentraleSupélec, CNRS, Université Paris-Saclay, 94235 Cachan, France

² Aix Marseille Univ, CNRS, Centrale Marseille, Institut Fresnel, F-13013 Marseille, France

³ American University of Technology, AUT Halat, Highway, Lebanon

the date of receipt and acceptance should be inserted later

Abstract. A model, based on classical mechanics and thermodynamics, is devised to investigate the properties of the current-driven, superconducting to normal transition. This process is shown to be reversible. Two different critical temperatures are introduced. The temperature dependence of the critical current is worked out and found to agree with observation. The peculiar transport properties of high- T_c compounds in the allegedly normal state and old magnetoelastic data are also interpreted within this framework. Several experiments are proposed to check the validity of this analysis.

PACS. 74.25.Bt Thermodynamic properties – 74.25.Fy Transport properties – 74.25.Ha Magnetic properties

1 Introduction

It has been argued recently[1] that feeding a growing current into a superconductor drives *continuously* superconducting electrons to normal ones. Besides, this process is reversible, i.e. decreasing the current back to 0 returns normal electrons to the superconducting state. Though such a first order transition has been extensively studied so far by applying a magnetic field[2,3,4,5,6,7,8], this work will be concerned rather with a theoretical account of the current

driven procedure, because, due to the Meissner effect[9] and the finite *ac* conductivity[4] in the superconducting state, the current density is spatially inhomogeneous and there is no one-to-one correspondence between the external magnetic field and the current distribution inside the sample. Furthermore, having high T_c compounds going normal requires a huge, often unpractical magnetic field[6,7,8]. All of these shortcomings are avoided in the current driven experiment.

The purpose of this work is twofold :

- this transition will be studied quantitatively with help of Newton’s law and thermodynamics;
- the resulting findings will be taken advantage of to shed light into the transport properties of high- T_c compounds in the non-superconducting state[6, 7, 8], muddled so far by countless conflicting[6, 7, 10] theories, and the magneto-elastic behaviour, observed in elementary superconductors[11, 12] for $T \leq T_c$ (T, T_c refer to temperature and critical temperature, respectively).

The outline is as follows : the electrodynamical and thermodynamical properties of the superconducting to normal transition are worked out in sections 2, 3, respectively; the T dependent critical current is discussed in section 4; this analysis is further applied to investigate the transport properties of high- T_c compounds in the "normal" state, in section 5; magneto-elastic data[11, 12] are discussed in section 6; the results of this work are summarized in the conclusion.

2 Electrodynamical discussion

As done previously[1, 9, 13, 14], our analysis will proceed within the two-fluid model. Accordingly, the conduction electrons make up a homogeneous mixture of normal and superconducting electrons, in concentration c_n, c_s , respectively. The normal electrons behave like a Fermi gas[15], characterised by T and the Fermi energy E_F . The Helmholtz free energy of independent electrons per unit volume F_n and E_F are related[15, 16] by $E_F = \frac{\partial F_n}{\partial c_n}$. By contrast, the

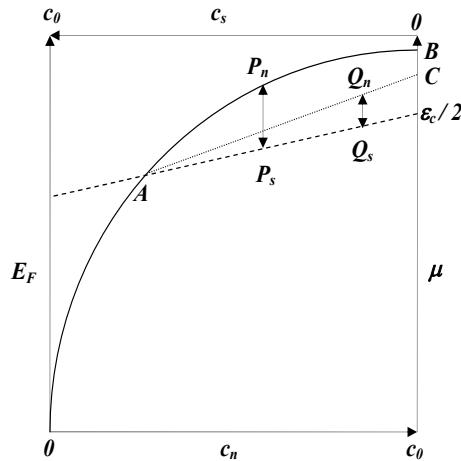


Fig. 1. schematic plots of $E_F(T < T_c, c_n)$ and $\mu(c_s)$ as solid and dashed lines, respectively; the origin $E_F = \mu = 0$ is set at the bottom of the conduction band; the tiny difference $E_F(T, c_n) - \mu(c_0 - c_n)$ has been hugely magnified for the reader’s convenience; the crossing point A between the solid and dashed lines represents the electron system in thermal equilibrium at T, T_* , according to Eq.(1); the isothermal process, addressed in sections 2, 3 is pictured by the P_n, P_s pair, whereas the dotted line and the Q_n, Q_s pair illustrate the adiabatic process, discussed in section 5

superconducting electrons are organised as a many bound electron state[1] of eigenenergy per unit volume $\mathcal{E}_s(c_s)$, such that its chemical potential reads $\mu = \frac{\partial \mathcal{E}_s}{\partial c_s}$. Gibbs and Duhem’s law[16] entails that the thermal equilibrium is characterised by

$$E_F(T, c_n(T)) = \mu(c_s(T)) \quad , \quad (1)$$

with $c_0 = c_n(T) + c_s(T)$ and c_0 being the concentration of conduction electrons.

Consider then a superconducting material of cylindrical shape, characterized by its symmetry axis z and radius r_0 in a cylindrical frame with coordinates (r, θ, z) and

flown through by a time dependent current $I(t) = \pi r_0^2 j(t)$, with $j(t)$ being a uniform current density. The analysis of an isothermal, current-driven, superconducting to normal transition, outlined elsewhere[1], will be developed below with $j(t) = \gamma t, \gamma > 0$. Accordingly, the initial state of the whole electron system is defined as $j(0) = 0, c_n = c_n(T), c_s = c_s(T)$ (see A in Fig.1). As $j(t)$ increases at constant T , the electron system shifts away from the equilibrium position in A : the Fermi gas, represented by P_n in Fig.1, moves, along the solid line, towards B , corresponding to the normal state $c_n = c_0$, while the superconducting electrons, represented by P_s , go, along the dashed line, towards the point characterized[1] by $\mu(c_s = 0) = \frac{\varepsilon_c}{2}$ (ε_c refers to the Cooper pair energy[18]). As this process will be shown to be reversible, the pair P_n, P_s , will shift back along the solid and dashed lines and will eventually merge into A , if j is brought back down to 0. A quantitative account of this process will be detailed below.

Due to $\gamma = \frac{dj}{dt} \neq 0$, Newton's law reads[1,9,13,14] for the normal and superconducting current densities $j_n(t), j_s(t)$ ($\Rightarrow j = j_n + j_s$)

$$\tau_n \frac{dj_n}{dt} = \sigma_n E - j_n \quad , \quad \tau_s \frac{dj_s}{dt} = \sigma_s (E - E_{s \rightarrow n}) - j_s. \quad (2)$$

E and τ_n, τ_s are, respectively, the applied electric field and the decay times of j_n, j_s , due to friction with the lattice, responsible for Ohm's law, whereas $\sigma_n = \frac{c_n e^2 \tau_n}{m}, \sigma_s = \frac{c_s e^2 \tau_s}{m}$ stand for the normal and superconducting conductivities[13, 14] ($\tau_n \ll \tau_s \Rightarrow \sigma_n \ll \sigma_s$) and m, e refer to the effective[15] mass and charge of an electron. The effective field $E_{s \rightarrow n}$ is defined with respect to $f_{s \rightarrow n} = c_s e E_{s \rightarrow n}$, the inter-electron force, which turns superconducting electrons into

normal ones. Actually $E_{s \rightarrow n}$ was neglected in previous[1, 9,13,14] works ($\Rightarrow j_s \approx \sigma_s E$). But, as it will appear below that $|\frac{E_{s \rightarrow n}}{E}| \ll 1$, such an approximation was fully vindicated.

During the elementary time-duration $\delta t, \delta c_s$ of superconducting electrons, moving at the mass center velocity[1, 9,13,14] v_s ($\Rightarrow v_s = \frac{j_s}{c_s e}$), are driven normal at vanishing velocity by $f_{s \rightarrow n}$, which corresponds to a momentum variation per unit volume of $\delta p = -m \delta c_s v_s$. Thence $f_{s \rightarrow n}$ is inferred from Newton's law to read

$$f_{s \rightarrow n} = \frac{\delta p}{\delta t} = -\frac{m \dot{c}_s}{c_s e} j_s \Rightarrow E_{s \rightarrow n} = -\frac{m \dot{c}_s}{(c_s e)^2} j_s \quad , \quad (3)$$

with $\dot{c}_s = \frac{dc_s}{dt}$. Then combining Eqs.(2,3), while recalling that the inertial force $\propto \frac{dj_s}{dt}$ is negligible[9,13], yields

$$E = \frac{j_n}{\sigma_n} = \frac{j_s}{\sigma_s} + E_{s \rightarrow n} \Rightarrow \frac{j_n}{\sigma_n} = \frac{j_s}{\sigma_s} = \frac{j}{\sigma_n + \sigma_s^*} \quad . \quad (4)$$

$$\sigma_s^* = \frac{\sigma_s}{1 - \tau_s \frac{\dot{c}_s}{c_s}}$$

Eq.(4) conveys the same meaning as Ohm's law, written for j_n, j_s flowing parallel to each other, except for the effective conductivity σ_s^* showing up instead of σ_s .

The elementary work δW , needed for one superconducting electron, moving with velocity v_s , to go normal with vanishing velocity, is reckoned to be equal to $\delta W = \frac{mv_s^2}{2} = \frac{m}{2} \left(\frac{j_s}{c_s e} \right)^2$, thanks to the kinetic energy theorem. On the other hand, for an isothermal process, δW is also equal to the difference of free energy[16] between the superconducting and normal states, which leads thence to the identity[16] $\delta W = \frac{\partial E_n}{\partial c_n} - \frac{\partial \mathcal{E}_s}{\partial c_s} = E_F(T, c_n) - \mu(c_s)$. Consequently, j_s reads finally

$$j_s(c_s) = c_s e \sqrt{\frac{2}{m} (E_F(T, c_0 - c_s) - \mu(c_s))} \quad . \quad (5)$$

Note that, unlike the normal current $j_n = \sigma_n E$, j_s is *independent* from the external field E and depends only on the *concentration* of bound electrons c_s .

Eq.(4) can now be recast as an ordinary differential equation of first order for the unknown $c_s(j)$

$$\gamma \frac{d \log c_s}{dj} = \frac{\frac{c_s}{c_n \tau_n} \left(\frac{j}{j_s(c_s)} - 1 \right) - \frac{1}{\tau_s}}{\frac{c_s}{c_n} \left(\frac{j}{j_s(c_s)} - 1 \right) - 1}, \quad (6)$$

with $c_n = c_0 - c_s$ and j_s given by Eq.(5).

For j increasing from 0, c_s decreases from $c_s(T)$, while $E_F - \mu$ increases from 0, proportionally to the length of the arrow linking P_n, P_s in Fig.1. In addition, since j_s will eventually vanish for $c_s \rightarrow 0$, as inferred from Eq.(5), j_s is bound to rise from $j_s = 0$ at A up to a maximum $j_s(c_m)$ at $c_m < c_s(T)$ defined by $\frac{dj_s}{dc_s}(c_m) = 0$. In order to solve Eq.(6), $E_F - \mu$ will be replaced by its Taylor's expansion at first order with respect to $c_s - c_s(T)$

$$\frac{e^2}{m} (E_F - \mu) = \beta (c_s(T) - c_s) \Rightarrow c_m = \frac{2}{3} c_s(T) \quad , \quad (7)$$

with $\beta = \frac{e^2}{m} \left(\frac{\partial E_F}{\partial c_n}(c_n(T)) + \frac{\partial \mu}{\partial c_s}(c_s(T)) \right)$. Thus Eq.(6) has been integrated with $c_0 = 10^{28}/m^3, c_s(T) = .1c_0, \tau_s = 10^{-9}s, \tau_n = 10^{-4}\tau_s, \beta = 10^{-65}A^2 \times m^5$ and initial condition $c_s(j = 0) = c_s(T)$. The resulting data $c_s(j), \sigma_e(j)$ ($\sigma_e = \sigma_n + \sigma_s^*$ refers to the effective conductivity) have been plotted in Figs.2,3, corresponding to $j \leq j_m$ or $j > j_m$, respectively, with j_m defined by $j_m = j_s(c_m)$.

For $j \leq j_m$, there is $\tau_s \left| \frac{\dot{c}_s}{c_s} \right| \ll 1$, so that Eq.(4) yields $\sigma_s^* \approx \sigma_s$ and Eq.(6) reduces to

$$\frac{j_s(c_s)}{j} = 1 + \frac{\sigma_n}{\sigma_s} = 1 + \frac{\tau_n}{\tau_s} \left(\frac{c_0}{c_s} - 1 \right) \quad . \quad (8)$$

Likewise, Eq.(8) implies $j_s \approx \sigma_s E \Rightarrow \left| \frac{E_{s \rightarrow n}}{E} \right| \ll 1$, which confirms the validity of a previous assumption. As γ does

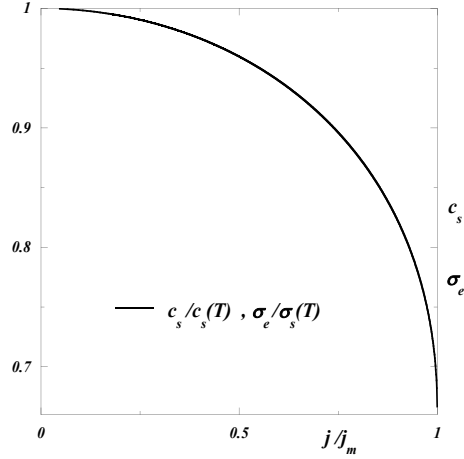


Fig. 2. plots of $c_s(j), \sigma_e(j)$ for $j \leq j_m$, as a solid line; the results have been found to be independent from γ in accordance with Eq.(8)

not show up in Eq.(8), there is a one-to-one correspondence between j and c_s , as seen in Fig.2. Moreover, $\tau_n \ll \tau_s$ entails that $j_s \approx j$, so that the $c_s(j), \sigma_e(j)$ plots cannot be distinguished from each other. Note that $\frac{dc_s}{dj}(j = 0) = 0$, while $\left| \frac{dc_s}{dj} \right|$ becomes very large for $j \rightarrow j_m$.

However, when j keeps growing beyond j_m , $j_s \approx j$ is no longer valid because of $j_s \leq j_m < j$. Consequently, as seen in Fig.3, $c_s(j)$, obtained by integrating Eq.(6) for $j > j_m$, falls steeply from $c_s(j_m) = c_m$ down to 0, and σ_e sinks by the ratio $\frac{c_s(T)\tau_s}{c_0\tau_n} = 10^3$ from $\sigma_e(T) \approx \sigma_s(T)$ down to $\sigma_e(T_c) = \frac{c_0 e^2 \tau_n}{m}$, typical of the normal metal. Meanwhile j undergoes a tiny increase from j_m up to j_M , with j_M being weakly γ dependent, i.e. $j_M/j_m - 1 \approx 10^{-7}, 10^{-8}$ for $\gamma = 2 \times 10^9, 2 \times 10^7 A/(m^2 \times s)$, respectively (see Fig.3). Finally, due to $j_M \approx j_m = j_s(c_m)$, $j_M(T < T_c)$ reads

$$j_M = e c_m \sqrt{\frac{2}{m} (E_F(T, c_0 - c_m) - \mu(c_m))} \quad .$$

Integrating Eq.(6) from $j = j_M$ down to $j = 0$ with the initial condition $c_s = c_s(j_M) \approx 0$, while keeping γ un-

altered, will produce the same solution $c_s(j)$, as displayed in Figs.2,3. This shows that the superconducting-normal transition is *reversible* and there is a *one-to-one* correspondence between j and c_s , provided that γ keeps the *same* value for j increasing from 0 up to j_M or decreasing from j_M down to 0, as well. This property holds actually for any $j(t)$, such that $j(t) = j(t_p - t), \forall t \in [0, t_p/2]$, with t_p taken such that $j(t_p/2) = j_M$.

Due to $j_s \approx j$ for $j < j_m$, measuring $\sigma_e(j)$ and the j dependent London length, which gives access[13,14] to c_s , would enable one to chart $E_F(T, c_n) - \mu(c_s)$ with help of Eq.(5). Given the highest observed j_M values, Eq.(5) provides the estimate $E_F(T, c_n) - \mu(c_s) < 10^{-5} eV$. It is noticeable that the conductivity, decreasing by several orders of magnitude for $j \rightarrow j_M$, as seen above, and for $T \rightarrow T_c^-$, as discussed elsewhere[14], is to be ascribed, in both cases, to c_s decreasing very steeply down to 0.

3 Thermodynamical discussion

As recalled above, the work $W_{s \rightarrow n}$, performed by $f_{s \rightarrow n}$, whereby all of superconducting electrons are turned into normal ones via an isothermal process[16], is equal to the difference of free energy per unit volume ΔF , between the normal and superconducting states. Due to the very definitions of E_F, μ , the work $W_{s \rightarrow n}$ is thence deduced to read

$$W_{s \rightarrow n} = \int_0^{c_s(T)} (E_F(T, c_0 - u) - \mu(u)) du \quad . \quad (9)$$

In addition, Eq.(9) implies that $W_{s \rightarrow n} = -W_{n \rightarrow s}$, consistently with the reversible nature of the transition.

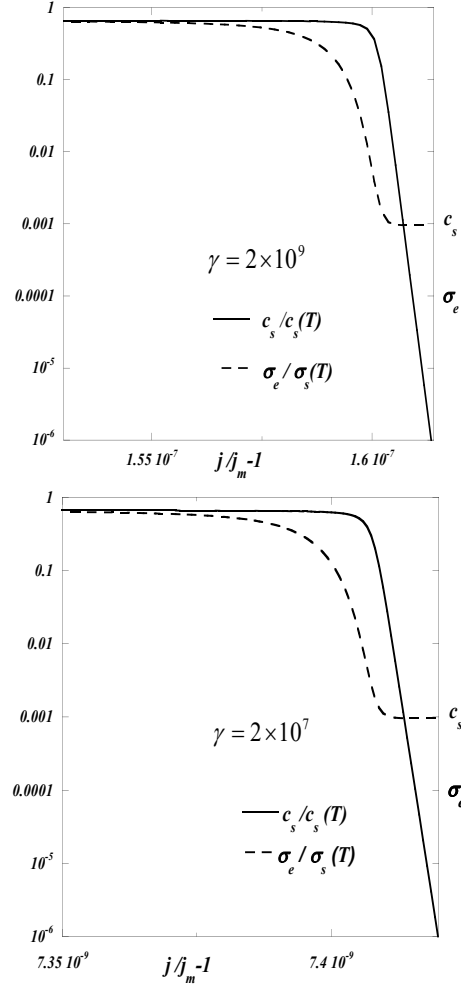


Fig. 3. plots of $c_s(j), \sigma_e(j)$ for $j > j_m$, as a solid and dashed line, respectively; the calculation has been done for two values $\gamma = 2 \times 10^7, 2 \times 10^9 A/(m^2 \times s)$

$W_{s \rightarrow n}$ can be also achieved alternatively by using the definition of $\Delta F = \Delta \mathcal{E} + T \Delta S$, with \mathcal{E}, S being, respectively, the total energy and entropy of the sample, i.e. including all of the *lattice* and *electron* degrees of freedom. $\Delta \mathcal{E}, \Delta S$ will be calculated by working out the detailed thermal balance over the following trajectory : the sample is first taken at $T < T_c$ and heated up to T_c with $j = 0$.

Hence, the associated $\Delta\mathcal{E}_1, \Delta\mathcal{S}_1$ read

$$\begin{aligned}\Delta\mathcal{E}_1 &= \int_T^{T_c} (C_\phi(u) + C_s(u)) du \\ \Delta\mathcal{S}_1 &= \int_T^{T_c} (C_\phi(u) + C_s(u)) \frac{du}{u}\end{aligned}, \quad (10)$$

with $C_\phi(T), C_s(T)$ standing for the respective contributions to the specific heat of the phonons (Debye) and of the conduction electrons in the superconducting state; then let the sample be cooled down back to T , while being flown through by a current density $j \geq j_M(T)$, so that the sample remains normal down to T . The associated $\Delta\mathcal{E}_2, \Delta\mathcal{S}_2$ read then

$$\begin{aligned}\Delta\mathcal{E}_2 &= \int_T^{T_c} (C_\phi(u) + C_n(u)) du \\ \Delta\mathcal{S}_2 &= \int_T^{T_c} (C_\phi(u) + C_n(u)) \frac{du}{u}\end{aligned}, \quad (11)$$

with $C_n(T)$ standing for the T linear, specific heat of a Fermi gas[15], which is known to be independent from j , like $C_\phi(T)$. At last, the searched expressions read

$$\begin{aligned}E_b(T) &= \Delta\mathcal{E}_1 + \Delta\mathcal{E}_2 = \int_T^{T_c} (C_s(u) - C_n(u)) du \\ W_{s \rightarrow n}(T) &= \Delta\mathcal{E}_1 + T\Delta\mathcal{S}_1 + \Delta\mathcal{E}_2 + T\Delta\mathcal{S}_2 \\ &= \int_T^{T_c} (C_s(u) - C_n(u)) \left(1 - \frac{T}{u}\right) du\end{aligned}, \quad (12)$$

with $E_b(T)$ being the binding energy of the superconducting phase with respect to the normal one at T . Noteworthy is that the superconducting phase being stable ($\Leftrightarrow E_b(T) > 0$) requires $C_s(T) > C_n(T)$ in Eq.(12), which is confirmed experimentally[2,15], i.e. $C_s(T_c) \approx 3C_n(T_c)$.

$W_{s \rightarrow n}$ can actually be measured directly by feeding a growing current $I(t) = \pi r_0^2 \gamma t$ into the superconducting sample, from $t = 0$ until $t = \frac{t_p}{2}$ with $I(\frac{t_p}{2}) = \pi r_0^2 j_M(T)$, so that the sample goes normal at $\frac{t_p}{2}$ (this is referred to as the Silsbee effect[2]). Then $I(t)$ is reduced, like $I(t) = \pi r_0^2 \gamma (t_p - t)$, from $I(\frac{t_p}{2})$ down to $I(t_p) = 0$. The work

$W(t_p)$, performed by the electric field E from $t = 0$ until $t = t_p$, reads then

$$W(t_p) = W_1 + W_2, \quad (13)$$

$$W_1 = \int_0^{\frac{t_p}{2}} U(t) I(t) dt, \quad W_2 = \int_{\frac{t_p}{2}}^{t_p} U(t) I(t) dt$$

with $U = El$ and l being the measured voltage drop across the sample and its length, respectively. Moreover, owing to Eq.(4), W_1, W_2 can be recast as

$$\begin{aligned}\frac{W_1}{\pi r_0^2 l} &= \int_0^{\frac{t_p}{2}} \left(\frac{j_n^2}{\sigma_n} + \frac{j_s^2}{\sigma_s} + j_s E_{s \rightarrow n} \right) dt \\ \frac{W_2}{\pi r_0^2 l} &= \int_{\frac{t_p}{2}}^{t_p} \left(\frac{j_n^2}{\sigma_n} + \frac{j_s^2}{\sigma_s} + j_s E_{n \rightarrow s} \right) dt\end{aligned}. \quad (14)$$

Likewise, recalling that $j_n, \sigma_n, j_s, \sigma_s$ have been shown above to depend on j only, if γ is kept fixed, and furthermore

$$\begin{aligned}W_{s \rightarrow n} &= \int_0^{\frac{t_p}{2}} j_s E_{s \rightarrow n} dt, \quad W_{n \rightarrow s} = \int_{\frac{t_p}{2}}^{t_p} j_s E_{n \rightarrow s} dt \\ W_{s \rightarrow n} &= -W_{n \rightarrow s}\end{aligned},$$

enables us to recast W_1, W_2 as

$$\begin{aligned}\frac{W_1}{\pi r_0^2 l} &= Q_1 + W_{s \rightarrow n}, \quad \frac{W_2}{\pi r_0^2 l} = Q_1 - W_{s \rightarrow n} \\ Q_1 &= \int_0^{j_M(T)} \left(\frac{j_n^2}{\sigma_n} + \frac{j_s^2}{\sigma_s} \right) \frac{dj}{\gamma}\end{aligned}, \quad (15)$$

with Q_1 expressing the Joule heat, released[1] through process I per unit volume for $t \in [0, t_p/2]$. Finally it ensues from Eq.(15)

$$\frac{W_1 - W_2}{2\pi r_0^2 l} = \int_T^{T_c} (C_s(u) - C_n(u)) \left(1 - \frac{T}{u}\right) du. \quad (16)$$

The validity of Eq.(16) should be checked experimentally first in a superconducting material, for which accurate data are available for C_s, C_n and thence T_c is low[15] enough for $C_s > C_\phi, C_n > C_\phi$. Accordingly, Al ($T_c = 1.19K$) might be a good candidate. In case of a successful test, Eq.(16) might then provide with a rather *unique* access to C_s in high T_c materials, for which the direct measurement of C_s proves unreliable[19], due to $C_s \ll C_\phi$.

Note that C_n can always be measured at low T by feeding into the sample a current density $j > j_M(T)$, whereby the sample goes normal even at $T < T_c$, because C_n is j independent, unlike C_s , and extrapolated further to higher T , by taking advantage of its T linear behaviour[15].

Although the superconducting to normal transition and ice melting into water are both first order processes, they differ in two respects :

- the role of the latent *heat*, typical of all usual first order transitions (melting or vaporisation), is played here by the latent *work* $W_{s \rightarrow n}$, because the superconducting-normal transition is controlled by *current* rather than by *temperature*;
- ice and water are separated by a clear-cut interface, whereas the mixture of superconducting and normal electrons is homogeneous. Consequently, the chemical potentials of ice and water remain uniquely defined all over the melting process, while E_F, μ vary continuously with $c_s \in [0, c_s(T < T_c)]$.

4 Critical current

As shown elsewhere[1], the *bound electron* current j_s will turn out to be *persistent*, only if the necessary condition $\sigma_s + \sigma_J > 0$, with $\sigma_J < 0$ being the conductivity characterising process II of the Joule effect, is fulfilled. It conveys the physical meaning that the negative Joule heat, released via the anomalous process II, typical of superconductors, should prevail over the positive one, stemming from the regular process I. Since σ_J reads[1] as

$\sigma_J = -\frac{(ev)^2 \tau_s}{\left| \frac{\partial \mu}{\partial c_s} \right|}$ with $mv^2 \approx 1eV$, the inequality $\sigma_s + \sigma_J > 0$ can be recast as

$$r(c_s) = \frac{c_s}{mv^2} \left| \frac{\partial \mu}{\partial c_s} \right| > 1 \quad . \quad (17)$$

As it will appear below that $\frac{\partial \mu}{\partial c_s}$ remains finite for $c_s \rightarrow 0$, the inequality (17) is bound not to hold any more for $c_s < c_c$ with the critical concentration c_c defined by $r(c_c) = 1$. To proceed further, c_c must be assessed, which requires to reckon $\frac{\partial \mu}{\partial c_s}$. The only practical tool for this purpose is the BCS scheme[17], but for some reason to become clear below, we shall refrain from using it, and rather develop our own procedure.

Thus let us consider a three-dimensional crystal containing N sites and $2n$ itinerant electrons with $N \gg 1, n \gg 1$ ($\Rightarrow c_s = 2n/N$). These electrons of spin $\sigma = \pm 1/2$ populate a single band, accomodating at most two electrons per site ($\Rightarrow n \leq N$). The independent electron motion is described, in reciprocal space, by the Hamiltonian H_d

$$H_d = \sum_{k, \sigma} \varepsilon(k) c_{k, \sigma}^+ c_{k, \sigma} \quad , \quad (18)$$

for which $\varepsilon(k), k$ are the one-electron, spin-independent energy ($\Rightarrow \varepsilon(k) = \varepsilon(-k)$) and a vector of the Brillouin zone, respectively, and the sum over k is to be carried out over the whole Brillouin zone. Then $c_{k, \sigma}^+, c_{k, \sigma}$ are one-electron creation and annihilation operators on the Bloch state $|k, \sigma\rangle$

$$|k, \sigma\rangle = c_{k, \sigma}^+ |0\rangle \quad , \quad |0\rangle = c_{k, \sigma} |k, \sigma\rangle \quad ,$$

with $|0\rangle$ being the no electron state. They enable us to introduce the two-electron creation and annihilation operators[17,

18,21] $b_{K,k}^+ = c_{k,+}^+ c_{K-k,-}^+$, $b_{K,k} = c_{K-k,-} c_{k,+}$. The interacting electron motion is governed by a truncated Hubbard Hamiltonian H_K , used previously[17,21]

$$H_K = \sum_k \varepsilon(K, k) b_{K,k}^+ b_{K,k} + \frac{U}{N} \sum_{k,k'} b_{K,k}^+ b_{K,k'} \quad , \quad (19)$$

with $\varepsilon(K, k) = \varepsilon(k) + \varepsilon(K - k)$ and U being the Hubbard coupling constant. Unlike previous authors[3,4,17,18], we shall consider *both* cases $U > 0, U < 0$.

The eigenstate of the Schrödinger equation, pertaining to a single bound pair, $(H_K - \varepsilon_c(K)) \varphi_c = 0$, is known as the Cooper pair[18] state $\varphi_c = \sum_k \frac{b_{K,k}^+}{\varepsilon_c(K) - \varepsilon(K, k)} |0\rangle$, with the eigenenergy $\varepsilon_c(K)$ being the solution of

$$\frac{1}{U} = \frac{1}{N} \sum_k \frac{1}{\varepsilon_c(K) - \varepsilon(K, k)} = \int_{-t_K}^{t_K} \frac{\rho_K(\varepsilon)}{\varepsilon_c(K) - \varepsilon} d\varepsilon. \quad (20)$$

$\pm t_K$ are the upper and lower bounds of the two-electron band, i.e. the maximum and minimum of $\varepsilon(K, k)$ over k , whereas $\rho_K(\varepsilon)$ is the corresponding two-electron density of states. For the sake of illustration, we shall solve Eq.(20) for $\rho_K(\varepsilon) = \frac{2}{\pi t_K} \sqrt{1 - \left(\frac{\varepsilon}{t_K}\right)^2}$, $t_K = t \cos(Ka/2)$, where t, a are the one-electron bandwidth and the lattice parameter, respectively. The dispersion curves $\varepsilon_c(K)$ are given in Fig.4 for $U > 0$ only, because it can be deduced from Eq.(20) and $\rho_K(\varepsilon) = \rho_K(-\varepsilon)$ that $\varepsilon_c(K, U) = -\varepsilon_c(K, -U)$. A remarkable feature is that $\varepsilon_c(K) \rightarrow t_K$, i.e. the upper bound of the two-electron band, for U decreasing toward $t_K/2$, so that there is *no* Cooper pair solution for $U < t_K/2$ (accordingly, the dashed curve is no longer defined in Fig.4 for $\frac{Ka}{\pi} < .13$), in marked contrast with the opposite conclusion reached elsewhere[18], that there is a Cooper pair, even for $U \rightarrow 0$. This discrepancy results from the three-dimensional Van Hove sin-

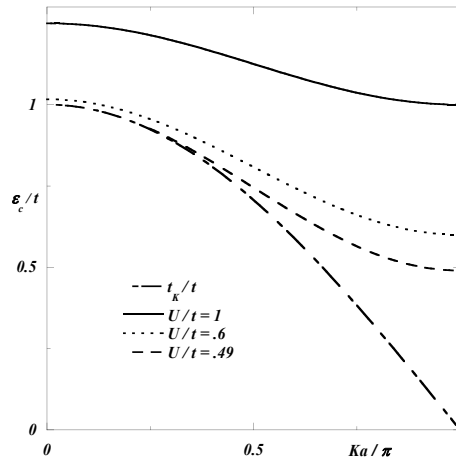


Fig. 4. dispersion curves of t_K as a dashed-dotted line and of $\varepsilon_c(K)$ as solid, dashed and dotted lines, associated with various U values, respectively

gularities, showing up at both two-electron band edges $\rho_K(\varepsilon \rightarrow \pm t_K) \propto \sqrt{t_K - |\varepsilon|}$, unlike the two-electron density of states, used previously[18], which displayed no such singularity.

H_K operates within the Hilbert space S_K . A typical vector of its basis reads $\varphi = \prod_{i=1, \dots, m} b_{K, k_i}^+ |0\rangle$ with m being any integer. We shall look for a variational approximation φ_v of the single[22,23] bound eigenstate of H_K inside the subset $\{\varphi_v\} \subset S_K$, characterized by

$$\langle \varphi_v | b_{K, k}^{(+)} | \varphi_v \rangle = (n_k (1 - n_k))^\alpha, \quad \forall \varphi_v \in \{\varphi_v\} \quad .$$

The real parameter α will be assigned shortly and $n_k = \langle \varphi_v | b_{K, k}^+ b_{K, k} | \varphi_v \rangle$. The pair number operator $b_{K, k}^+ b_{K, k}$ has two eigenvalues 0, 1, associated with $|0\rangle$ and $b_{K, k}^+ |0\rangle$, respectively, so that $0 \leq n_k \leq 1$ and $\sum_k n_k = n$. The energy of φ_v per site reads

$$\mathcal{E} = \frac{\langle \varphi_v | H_K | \varphi_v \rangle}{N} = \sum_k \varepsilon(K, k) \frac{n_k}{N} + U \Delta^2$$

$$\Delta = \sum_k \frac{(n_k (1 - n_k))^\alpha}{N}$$

Hence minimising \mathcal{E} ($\Rightarrow d\mathcal{E} = 0$), under the constraint of n kept constant ($\Rightarrow dn = 0$), yields

$$\varepsilon(K, k) + 2\alpha U \Delta \frac{1 - 2n_k}{(n_k(1 - n_k))^{1-\alpha}} = \lambda \quad ,$$

with $\lambda = \frac{\partial \mathcal{E}}{\partial n_k}$, $\forall k$ being a Lagrange multiplier, which implies that $\lambda = \frac{\partial \mathcal{E}}{\partial n} = 2\mu(c_s = \frac{2n}{N})$. The α value will be assigned now by checking consistency with the Cooper pair properties in the limit $n \rightarrow 0 \Rightarrow n_k \rightarrow 0 \Rightarrow n_k \propto (2\mu - \varepsilon(K, k))^{\frac{1}{\alpha-1}}$. Comparing with $n_k = \langle \varphi_c | b_{K,k}^+ b_{K,k} | \varphi_c \rangle \propto (\varepsilon_c(K) - \varepsilon(K, k))^{-2}$, inferred from Eq.(20), yields finally $\alpha = 1/2$ and $\varepsilon_c(K) = 2\mu(c_s = 0)$, a conclusion which had already been reached by an independent rationale[1]. Hence, our variational procedure can be summarised, with help of notations introduced elsewhere[3], as follows

$$\tan 2\theta_k = \frac{2U\Delta}{2\mu - \varepsilon(K, k)} \quad , \quad n_k = \sin^2 \theta_k$$

$$\Delta = \sum_k \frac{\sin 2\theta_k}{2N} = \int_{-t_K}^{t_K} \frac{\sin 2\theta(\varepsilon)}{2} \rho_K(\varepsilon) d\varepsilon \quad , \quad (21)$$

$$c_s = 2 \sum_k \frac{\sin^2 \theta_k}{N} = 2 \int_{-t_K}^{t_K} \sin^2 \theta(\varepsilon) \rho_K(\varepsilon) d\varepsilon$$

with $0 \leq \theta_k \leq \frac{\pi}{2}$. The formulae in Eqs.(21) are found to be identical to those of BCS[3,4,17]. As an illustrative example, Eqs.(21) have been solved for $\mu(c_s)$, $\Delta(c_s)$ and $r(c_s)$ defined by Eq.(17), with $U > 0$ and $c_s < 1$ electron per site, only, because it can be deduced from Eqs.(21) and $\rho_K(\varepsilon) = \rho_K(-\varepsilon)$ that $\mu(c_s, U) = -\mu(c_s, -U) = -\mu(2 - c_s, U)$. The results, presented in Fig.5, exhibit $\frac{\partial \mu}{\partial c_s}$ almost independent from c_s and $\Delta(c_s \rightarrow 0) \propto \sqrt{c_s}$. An important inequality, holding for $U > 0$ and $U < 0$ as well, can be deduced from $\mu(c_s, U) = -\mu(c_s, -U)$ and Fig.5

$$U \frac{\partial \mu}{\partial c_s} < 0 \quad . \quad (22)$$

Note that for $K = \frac{\pi}{a}$, the two-electron band is dispersionless because of $t_{K=\frac{\pi}{a}} = 0$. Then applying Eqs.(21)

to the $K = \frac{\pi}{a}$ case gives $\Delta = \frac{\sin 2\theta}{2}$ and finally $\mu = \frac{U}{2}(1 - c_s)$, the validity of which can be checked independently, because the n -pair, bound eigenstate of $H_{K=\frac{\pi}{a}}$ is known[21] to read $\varphi = \sum_{i=1, \dots, d} \frac{\varphi_i}{\sqrt{d}}$, with $d = \binom{N}{n}$, $\varphi_i = \prod_{l=1, \dots, n} b_{\frac{\pi}{a}, k_{i_l}}^+ |0\rangle$ and the sum with respect to i runs over all of n pair combinations $\{b_{\frac{\pi}{a}, k_{i_1}}^+, \dots, b_{\frac{\pi}{a}, k_{i_n}}^+\}$, chosen among N of available pairs. As each φ_i contributes $\frac{n}{dN}(1 - \frac{n}{N})U$ to \mathcal{E} , it can thence be inferred $\mathcal{E} = U \frac{c_s}{2}(1 - \frac{c_s}{2}) \Rightarrow \mu = \frac{\partial \mathcal{E}}{\partial c_s} = \frac{U}{2}(1 - c_s)$, which is seen to be identical to the above result, deduced from Eqs.(21). At last, there is $U \frac{\partial \mu}{\partial c_s} = -U^2/2 < 0$ in accordance with inequality (22).

Combining Eq.(20) with Taylor's expansions of $\sin 2\theta_k$, $\sin^2 \theta_k$, worked out from Eqs.(21), up to Δ^2 for $c_s \rightarrow 0 \Rightarrow \Delta \rightarrow 0$, leads to

$$\frac{1}{U} = \int_{-t_K}^{t_K} \frac{\rho_K(\varepsilon)}{\varepsilon_c(K) - \varepsilon} d\varepsilon$$

$$= \int_{-t_K}^{t_K} \left(1 - 2 \left(\frac{U\Delta}{2\mu - \varepsilon} \right)^2 \right) \frac{\rho_K(\varepsilon)}{2\mu - \varepsilon} d\varepsilon \quad .$$

$$(U\Delta)^2 = \frac{c_s}{2 \int_{-t_K}^{t_K} \frac{\rho_K(\varepsilon)}{(\varepsilon_c(K) - \varepsilon)^2} d\varepsilon}$$

Subtracting the integrals equal to $1/U$ from each other, while taking advantage of $\mu(c_s \rightarrow 0) \rightarrow \varepsilon_c(K)/2$, gives in turn

$$(U\Delta)^2 = \left(\frac{\varepsilon_c(K)}{2} - \mu \right) \frac{\int_{-t_K}^{t_K} \frac{\rho_K(\varepsilon)}{(\varepsilon_c(K) - \varepsilon)^2} d\varepsilon}{\int_{-t_K}^{t_K} \frac{\rho_K(\varepsilon)}{(\varepsilon_c(K) - \varepsilon)^3} d\varepsilon} \quad .$$

Equating both expressions of $(U\Delta)^2$ yields finally

$$\frac{\partial \mu}{\partial c_s}(K, c_s = 0) = - \frac{\int_{-t_K}^{t_K} \frac{\rho_K(\varepsilon)}{(\varepsilon_c(K) - \varepsilon)^3} d\varepsilon}{2 \left(\int_{-t_K}^{t_K} \frac{\rho_K(\varepsilon)}{(\varepsilon_c(K) - \varepsilon)^2} d\varepsilon \right)^2} \quad .$$

Note that $\left| \frac{\partial \mu}{\partial c_s}(K, c_s = 0) \right| \rightarrow \infty$ for $U \rightarrow t_K/2$ and $U \frac{\partial \mu}{\partial c_s}(K, c_s = 0) < 0$ in accordance with inequality (22).

With help of Fig.5, c_c , defined by $r(c_c) = 1$ in Eq.(17), can now be assigned, for $K = 0$, to the values .7, .54, and

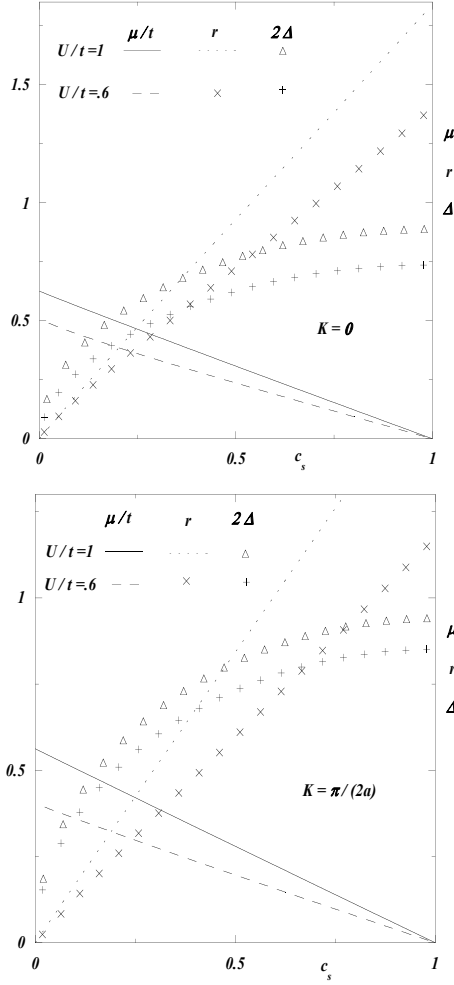


Fig. 5. plots of $\mu(c_s), \Delta(c_s), r(c_s)$ reckoned for $K = 0, \frac{\pi}{2a}$; the solid and dotted lines and the triangles, which pertain to μ, r, Δ , respectively, have been calculated with $U/t = 1$, whereas the dashed line and the $\times, +$ symbols, which refer to μ, r, Δ , respectively, have been calculated with $U/t = .6$; the r data have been calculated with $mv^2 = t/3$; $c_s = 1$ corresponds to one electron per site

for $K = \frac{\pi}{2a}$, to the values .85, .6, associated with $U/t = .6, 1$, respectively. Noteworthy is that φ_v will sustain persistent currents or not, according to whether $c_s > c_c$ or $c_s < c_c$, although φ_v undergoes *no qualitative* change for $c_s = c_c$. Accordingly, it still obeys Eqs.(21) for $c_s > c_c$ and $c_s < c_c$, as well. Therefore, $\varphi_v(c_s < c_c)$ will be referred to

below, as the many-bound-electron, *non-superconducting* (MBENS) state. Moreover, applying Eq.(5) for $c_s = c_c$, while taking advantage of the Sommerfeld integral[15] and Eq.(1), yields the critical current density as

$$j_c(T) = c_c e \sqrt{\frac{2}{m} (E_F(T, c_0 - c_c) - \mu(c_c))} \quad (23)$$

$$= \pi k_B e c_c \sqrt{\frac{\rho'(E_F^*)}{3m\rho(E_F^*)} (T_*^2 - T^2)}$$

with $E_F^* = E_F(T_*, c_0 - c_c)$. $k_B, \rho(\varepsilon)$ designate Boltzmann's constant and the one-electron density of states and $\rho'(\varepsilon) = \frac{d\rho}{d\varepsilon}$, while $T_* < T_c$ is defined by $E_F(T_*, c_0 - c_c) = \mu(c_c) \Rightarrow c_s(T_*) = c_c$. The calculated behavior $j_c(T) \propto \sqrt{T_*^2 - T^2}$, resulting from Eq.(23), is found to agree with observation[3, 4, 5, 15]. Consequently, the MBENS state and the superconducting one can be observed for $T_* < T < T_c$ and $T < T_*$, respectively. In low T_c compounds, $T_c - T_*$ is likely to be so small that T_c, T_* cannot be resolved experimentally from each other. However $T_c - T_*$ will be argued in the next section to be quite sizeable in high T_c materials.

$\frac{\partial \mu}{\partial c_s} < 0$ has been shown[1] to be a prerequisite for persistent currents. Hence, the inequality 22 entails $U > 0$. Besides, an additional setback of the assumption[17, 18] $U < 0 \Rightarrow \frac{\partial \mu}{\partial c_s} > 0$ is to preclude any thermal equilibrium for $T < T_c$. Here is a proof by contradiction. Let us assume that the BCS state is indeed in equilibrium at T_c , which implies $E_F(T_c, c_0) = \mu(c_s = 0)$, because of $c_s(T_c) = 0, c_n(T_c) = c_0$, in accordance with Eq.(1). When T decreases from T_c down to 0, charge conservation $c_0 = c_n(T) + c_s(T)$ entails

$$E_F(T) = E_F(T_c) - \frac{c_s(T)}{\rho(E_F(T_c))}, \quad \mu(T) = \mu(T_c) + \frac{\partial \mu}{\partial c_s} c_s(T),$$

for which we have used[15] $\frac{\partial E_F}{\partial c_s} = 1/\rho(E_F)$, while neglecting $\frac{\partial E_F}{k_B \partial T} \approx k_B T/E_F \ll 1$. Thus, $\frac{\partial \mu}{\partial c_s} > 0$ implies $E_F(T) < E_F(T_c) = \mu(T_c) < \mu(T)$, so that the equilibrium condition $\mu(c_s(T)) = E_F(T, c_0 - c_s(T))$ in Eq.(1) cannot be fulfilled for any $T < T_c$. *Q.E.D.*

5 High- T_c compounds

Overdoped high T_c compounds are known[6,7,8] to undergo, at some temperature T_0 , a crossover from a superconducting state of type II, observed for $T < T_0$, to a metallic state, displaying peculiar conduction properties up to $T \gg T_0$:

- contrary to the conductivity expected to be low, given the high doping rate $> .15$, it is observed to be large;
- the Hall coefficient is found to be T dependent, which hints at a T dependent carrier concentration, unlike what is observed in usual metals and alloys, behaving like a Fermi gas[15] with T independent concentration.

Both above mentioned features might be consistent with an electron system, comprising a Fermi gas *and* a MBENS state at thermal equilibrium fulfilling Eq.(1), in respective concentration $c_n(T > T_0), c_s(T)$ with $c_0 = c_n(T) + c_s(T)$. As a matter of fact, $\tau_s \gg \tau_n$ entails[13] that the large conductivity is settled by the MBENS electrons only and the Hall coefficient, dominated by j_s , is T dependent as is $c_s(T)$. The main virtue of such an assumption is that it lends itself to an experimental check, as shown below.

Consider a thermally isolated sample, flown through by $I(t) = \pi r_0^2 j(t)$ with $j(t) = \gamma t$, and taken at $t = 0$ in the

thermal equilibrium state, represented by A in Fig.1, i.e. $T(t = 0) = T_*, I(t = 0) = 0, c_n(t = 0) = c_n(T_*), c_s(t = 0) = c_0 - c_n(T_*)$. While $I(t)$ keeps growing, the bound electrons, pictured by Q_s in Fig.1, are turned into independent ones, depicted by Q_n , as explained in section 2. The experiment ends up at $t = t_f$, when Q_n , after traveling all along the dotted line, merges with C , referring to the normal state and thence characterized by $T(t_f) = T_f, c_n(t_f) = c_0, c_s(t_f) = 0$. Thus applying the first law of thermodynamics to this adiabatic process yields

$$\int_{T_*}^{T_f} C_\phi(T) dT = Q_1 + Q_2 \quad , \quad Q_2 = \int_0^{t_f} \frac{j_s^2(t)}{\sigma_J} dt \quad , \quad (24)$$

$$Q_1 = \int_0^{t_f} \frac{U(t)}{l} j(t) dt = \int_0^{t_f} \left(\frac{j_n^2(t)}{\sigma_n} + \frac{j_s^2(t)}{\sigma_s} \right) dt$$

where $Q_1 > 0, Q_2 < 0$ stand for the Joule heat released through processes[1] I and II, respectively, and $C_n(T > T_*) \ll C_\phi(T), C_s(T > T_*) \ll C_\phi(T), W_{s \rightarrow n} \ll Q_1$ have been neglected. Derivating Eq.(24) with respect to t gives finally

$$C_\phi(T) \dot{T} = \frac{U(t)}{l} j(t) + \frac{j_s^2}{\sigma_J} = \frac{j_n^2}{\sigma_n} + j_s^2 \left(\frac{1}{\sigma_s} + \frac{1}{\sigma_J} \right) \quad , \quad (25)$$

with $\dot{T} = \frac{dT}{dt}$. Because of $\frac{1}{\sigma_s} + \frac{1}{\sigma_J} > 0$, due to the very definition of T_* , we predict $\dot{T} > 0 \Rightarrow T_f > T_*$, with $\sigma_J < 0 \Rightarrow C_\phi(T) \dot{T} < \frac{U(t)}{l} j(t), \forall t$. Although the Joule effect is seen to warm up the sample, as occurs in a usual metal, it should be noticed that the same experiment, carried out at $T > T_c$ or equivalently in a normal conductor, would result rather into $C_\phi(T) \dot{T} = \frac{U(t)}{l} j(t), \forall t$. Conversely, would the experiment be performed at $T < T_* \Rightarrow \frac{1}{\sigma_s} + \frac{1}{\sigma_J} < 0$, we should observe[1] $\dot{T} < 0$, as remarked by De Gennes too (see[5] footnote in p.18). At last, due to the high doping rate, the local electron concentration is likely to display

spatial fluctuations, which should eventually result into a sample, comprising both superconducting *and* MBENS domains. This case could be brought to experimental evidence by observing different thermal balances in Eq.(25), while feeding either a *dc* or *ac* current into the sample, because superconducting domains will contribute to the Joule effect *only* for *ac* current, whereas MBENS ones will do in *both* cases.

6 Magnetoelasticity

Magnetoelastic effects were reported[11,12] long ago, in superconducting metals, undergoing a magnetic field H at $T \leq T_c$ and atmospheric pressure : when H starts growing from 0, the sample first expands by a tiny amount ($\approx 10^{-7}$) and then shrinks abruptly for H reaching some critical value $H_c(T)$, at which the sample goes normal. Actually, because the superconducting electrons are known[2, 3,4,5] to be in a macroscopic singlet spin state, H has no direct sway on them, but merely induces an eddy current according to Faraday's law[9]. This current, responsible for the Meissner effect, turns superconducting electrons into normal ones, as discussed in section 2, but only within a thin film of thickness λ_M , located at the outer edge of the sample[9]. Meanwhile, the partial pressure, stemming from the electrons, is altered, as will be shown now.

The free energy, associated with a sample of volume V , containing n conduction electrons ($\Rightarrow \frac{n}{V} = c_0 = c_n + c_s$), reads $VF(T, c_0)$ with $F(T, c_0) = F_n(T, c_n) + \mathcal{E}_s(c_s)$ being the electronic free energy per unit volume. The partial

pressure p_e , exerted by the electrons, reads[16] then

$$p_e(H \neq 0) = -\frac{\partial(VF)}{\partial V} = c_0 \frac{\partial F}{\partial c_0} - F, \quad (26)$$

$$= c_n E_F(T, c_n) - F_n + c_s \mu(c_s) - \mathcal{E}_s$$

with $c_n > c_n(T)$, $F_n = \int_0^{c_n} E_F(T, u) du$, $c_s = c_0 - c_n$, $\mathcal{E}_s = \int_0^{c_s} \mu(u) du$.

Eq.(26) implies

$$\frac{\partial p_e}{\partial c_n} = c_n \frac{\partial E_F}{\partial c_n} - c_s \frac{\partial \mu}{\partial c_s}.$$

Besides, $\frac{\partial E_F}{\partial c_n} = \frac{1}{\rho(E_F)}$, $\frac{\partial \mu}{\partial c_s} < 0$ entail $\frac{\partial p_e}{\partial c_n} > 0$. Since c_n grows at the expense of c_s for increasing H , the inequality $\frac{\partial H}{\partial c_n} > 0$ is always valid, which implies at last $\frac{\partial p_e}{\partial H} > 0$, in agreement with the observed H induced expansion[11,12].

For $H = H_c(T)$, the sample goes normal, so that H penetrates suddenly into bulk matter and polarises the whole set of normal electrons in concentration c_0 . The associated paramagnetic energy per unit volume reads[15] $\mathcal{E}_H = -\frac{(\mu_B H)^2}{2} \rho(E_F(T, c_0))$ with μ_B being the Bohr magneton. Because Pauli's susceptibility is T independent[15], \mathcal{E}_H is also equal to the magnetic contribution to the free energy, so that the partial pressure p_H , associated with H , reads

$$p_H = c_0 \frac{\partial \mathcal{E}_H}{\partial c_0} - \mathcal{E}_H = \frac{(\mu_B H)^2}{2} \left(\rho(E_F) - c_0 \frac{\rho'(E_F)}{\rho(E_F)} \right),$$

with $E_F = E_F(T, c_0)$. As the sample was reported[11,12] to shrink at $H_c(T)$, this implies $p_H < 0$, which can be realized only if $E_F(T, c_0)$ lies close to a Van Hove singularity at $\varepsilon_{VH} \Rightarrow \rho'(E_F) \propto |E_F - \varepsilon_{VH}|^{-1/2} \gg 1$.

This kind of H driven experiment provides merely qualitative information, because of several drawbacks, related to the Meissner effect[9], as recalled in section 1. Consequently, the critical field $H_c(T)$ is ill-defined. To buttress

this conclusion, we shall calculate $H(r)$ induced by the homogeneous current density j_c , parallel to the z axis. $H(r)$ is normal[9] to the unit vectors along the r and z coordinates and there is $H = rj_c/2$, thanks to the Ampère-Maxwell equation. Hence, H is seen to vary from $H(r=0) = 0$ up to $H(r_0) = r_0j_c/2$, so that H_c cannot be defined in a *unique* way, unlike $j_c(T)$. Likewise superconductors of type II make this proof more cogent, inasmuch as the whole superconducting sample is known[2,3,4,5] to turn continuously normal over a *broad* range of critical values $H_c \in [H_{c1}, H_{c2}]$ with $H_{c1} \ll H_{c2}$.

7 Conclusion

The physical significance of two different critical temperatures T_*, T_c with $T_* < T_c$, characterizing the electro-dynamical behavior of superconducting materials, has been analyzed. Whereas no persistent current can be observed for $T > T_*$, T_c is the upper bound of the MBENS state ($\Leftrightarrow c_s(T \geq T_c) = 0$) and is also identical to the usual critical temperature. The expression of the maximum persistent current $j_c(T)$ has been worked out and found to agree with observation. Besides, $j_c(T < T_*)$ can be observed *only* if $c_m < c_c$. Unlike the normal current j_n , the bound electron current j_s does not depend on the applied electric field, but rather on c_s and contributes a *cooling* part to the Joule effect[1], whether $c_s < c_c$ or $c_s > c_c$. The many-body wave-function, describing the motion of bound electrons, is identical for both superconducting *and* MBENS states, and accurately approximated by the BCS variational scheme. Conversely, the critical field H_c has

been shown to lack a unique definition. Whereas T_*, T_c are unlikely to be resolved from each other in conventional superconductors, T_c/T_* may be > 10 in high T_c compounds. Moreover, their peculiar conduction properties in the controversial[10] range $T \in [T_*, T_c]$ have been ascribed to a MBENS state and an experiment has been outlined to check the validity of this assumption. Another experiment has been proposed to measure the electronic specific heat in a T range, for which it is overshadowed by the lattice contribution. The advantage of a current driven experiment over a H driven one has been emphasized. At last, it has been shown that a *repulsive* ($U > 0$) Hubbard coupling is a prerequisite for superconductivity at thermal equilibrium, in accordance with the Coulomb force and Eq.(1).

References

1. Szeftel, J. and Sandeau, N. and Abou Ghantous, M. An observable prerequisite for the existence of persistent currents. *Eur.Phys.J. B* **2019** 92, 67.
2. Parks, R.D. *Superconductivity*; ed. CRC Press, 1969.
3. Tinkham, M. *Introduction to Superconductivity*; ed. Dover Books, 2004.
4. Schrieffer, J.R. *Theory of Superconductivity*; ed. Addison-Wesley, 1993.
5. De Gennes, P.G. *Superconductivity of Metals and Alloys*; ed. Addison-Wesley, Reading, MA, 1989.
6. Anderson, P.W. *The Theory of Superconductivity in High T_c Cuprates*; ed. Princeton University Press, NJ, 1995.

7. Armitage, N. P. and Fournier, P. and Greene, R. L. Progress and perspectives on electron-doped cuprates. *Review of Modern Physics* **2010** *82*, 2421-2487.
8. Ando, Y. and Boebinger, G.S. and Passner, and Kimura, T. and Kishio, K. Logarithmic Divergence of both In-Plane and Out-of-Plane Normal-State Resistivities of Superconducting $La_{2-x}Sr_xCuO_4$ in the Zero-Temperature Limit. *Phys.Rev.Lett.* **1995** *75*, 4662-4666.
9. Szeftel, J. and Sandeau, N. and Khater, A. Comparative Study of the Meissner and Skin Effects in Superconductors. *Prog.In.Electro.Res.M* **2018** *69*, 69-76.
10. Lederer, P. The battle of High Temperature Superconductivity, *arXiv:1510.0880* **2016**.
11. Olsen, J.L. and Rohrer, H. The Volume Change at the Superconducting Transition . *Helv. Phy. Acta* **1957** *30*, 49.
12. Olsen, J.L. and Rohrer, H. The volume dependence of the electron level density and the critical temperature in superconductors. *Helv. Phy. Acta* **1960** *33*, 872.
13. Szeftel, J. and Sandeau, N. and Khater, A. Study of the skin effect in superconducting materials. *Phys.Lett.A* **2017** *381*, 1525-1528.
14. Szeftel, J. and Abou Ghantous M. and Sandeau, N. Revisiting low-frequency susceptibility data in superconducting materials. *Prog.In.Electro.Res.L* **2019** *81*, 1-8
15. Ashcroft, N.W. and Mermin, N. D. *Solid State Physics*; ed. Saunders College, 1976.
16. Landau, L.D. and Lifshitz, E.M. *Statistical Physics*; ed. Pergamon Press, London, 1959.
17. Bardeen, J. and Cooper, L.N. and Schrieffer, J.R. Theory of superconductivity. *Phys. Rev.* **1957** *108*, 1175.
18. Cooper, L.N. Bound electron pairs in a degenerate Fermi gas. *Phys. Rev.* **1956** *104*, 1189.
19. Loram, J.W. and Mirza, K.A. and Freeman, P.F. The electronic specific heat in $YBa_2(Cu_{1-x}Zn_x)_3O_7$ from 1.6K to 300K. *Physica C* **1990** *171*, 243-256.
20. Ginzburg, V.L. and Landau, L.D. On superconductivity theory *Zh. Eksperim. i. Teor. Fiz.* **1950** *1064*, 20.
21. Szeftel, J. and Khater, A. Some properties of the eigenstates in the many-electron problem. *Phys.Rev.B* **1996** *54*, 13581.
22. Szeftel, J. Spin permutation at work in the BCS Hamiltonian. *Electron Correlations and Material Properties 2*; eds. A. Gonis, N. Kioussis, M. Ciftan (Kluwer Academic, New York), 2003.
23. Szeftel, J. and Caffarel, M. Block-diagonalization of the BCS Hamiltonian using spin-transpositions. *J.Phys. A* **2004** *37*, 623.